# A Comparative Study of As, Sb and P-based Metamorphic HEMT

D. Lubyshev, W. K. Liu, T. Stewart, A.B. Cornfeld, J. Patton*, J. Mirecki Millunchick*, W. Hoke**, C. Meaton§, K. Nichols†, and S.P. Svensson‡

Quantum Epitaxial Designs, Inc, Bethlehem, PA 18015, USA, **(610) 861-6930, dmitri@qedmbe.com**
*Department of Materials Science and Engineering, University of Michigan, Ann Arbor, MI 48109, USA
**Raytheon Microelectronics Center, Andover, MA 01810, USA
§Epitaixal Products International, Ltd., Cardiff, United Kingdom
†Sanders, A Lockheed Martin Company, Nashua, NH 03061 USA
‡Army Research Laboratory, College Park, MD 20740, USA

## Abstract

**Metamorphic HEMT (MHEMT) structures on As, Sb, and P-based buffers with different grading profiles were grown by molecular beam epitaxy. Structural, electrical, and optical characterization were used to correlate buffer layer design and growth parameters with channel carrier mobility, surface morphology, and photoluminescence efficiency. All MHEMTs studied in this work exhibited excellent transport properties comparable to reference HEMT grown lattice-matched on InP. RMS roughness of <14 Å were achieved for both InAlGaAs and AlGaAsSb-based buffers. MHEMT devices with 0.15 μm gates was fabricated successfully with transconductance of 710 mS/mm, maximum current of 500 mA/mm, and gate-drain breakdown of 5 V.**

## INTRODUCTION

The electronic transport properties of field effect transistors (FETs) with InGaAs channels are known to benefit by increasing the In content in the channel region. InP-based HEMTs, with In mole fractions x(In) equal to 0.53 in the channel, exhibit superior performance in microwave and millimeter wave applications compared to their GaAs counterparts which utilize x(In)~0.20. Unfortunately, this improved device performance comes with a price due to the higher substrate cost and lower processing yield compared to GaAs-based technology. In additional, GaAs substrates are available in larger diameters than InP substrates; larger diameter substrates enable device fabrication yield enhancement and cost reduction.

To combine the advantages of GaAs substrates with high In mole fraction channels, various partially-relaxed buffer layer schemes known as metamorphic buffers (M-buffers) have been used to grow InGaAs/InAlAs HEMT structures (metamorphic HEMTs, or MHEMTs) on GaAs substrates. The two most common approaches are the As-based InAlAs graded-buffer and Sb-based AlGaAsSb graded-buffer. The basic concept is to grade the buffer layer composition such that the lattice constant can be shifted from that of the substrate to that of the active layer, while maintaining high buffer layer resistivity, a smooth growth front, and with minimal dislocation propagation into the active layer.

The purpose of this work is to evaluate different M-buffer schemes on GaAs substrates in order to attain HEMT device performance that equals or exceeds that of InP-based HEMTs (LM-HEMT). M-buffers studied include graded InAl(Ga)As, InAlP, and AlGaAsSb layers. Emphasis will be placed on correlating buffer layer design and growth parameters with channel carrier mobility, surface morphology, and photoluminescence efficiency. DC characteristics of processed MHEMT devices will also be discussed.

## EXPERIMENTAL

All samples discussed in this work were grown on 3-inch diameter 2° off (100) substrates using a solid-source Varian GENII MBE system equipped with As and P valved-crackers. Compositionally graded InAl(Ga)As layers were grown using large capacity In and Ga SUMO cells (EPI). In flux measurements during simulated growth of graded buffer produced good correlation between real In flux and expected In composition profile. Growth temperature was calibrated using an optical pyrometer. The MHEMT samples were characterized using various techniques. Lattice mismatch parallel to the growth direction was measured by a 5-crystal Philips high-resolution x-ray diffraction system (HRXRD) using the (004) reflection. Electrical properties were determined by Hall-effect measurement with van der Pauw geometry at 300 and 77 K. Surface roughness analysis was performed using tapping-mode atomic force microscopy (AFM, Digital

Instrument NanoScope). A root-mean-square (RMS) roughness of 20 Å (based on a 5µm×5µm scan) is generally accepted as the figure of merit for gauging device reliability. Room temperature photoluminescence (PL) data was obtained using a Bio-Rad RMP2000 system.

The nominal single pulsed-doped HEMT structure with a 53.2% InGaAs channel, grown lattice-matched on InP (reference sample) and on M-buffer/GaAs substrate, is shown schematically in Fig. 1. Three different M-buffer schemes were studied, including: (A) a 1.1 µm InAl(Ga)As M-buffer, (B) a 1.1 µm InAlP M-buffer, and (C) a 1.8 µm AlGaAsSb M-buffer.

FIGURE 1
SCHEMATIC CROSS-SECTION OF MHEMT STRUCTURE

| |
|---|
| n+ InGaAs cap |
| undoped InAlAs Schottky layer |
| Si pulsed-doped layer<br>$[n]=3\text{–}5\times10^{12}\,\text{cm}^{-2}$ |
| undoped InAlAs spacer |
| undoped InGaAs QW |
| undoped InAlAs |
| LM or MM (As, P, and Sb-based) buffer |
| InP or GaAs substrate |

## MATERIAL CHARACTERIZATION

### (A) AS-BASED MHEMT

Our nominal As-based M-buffer consists of a linearly graded InAlAs layer and an inverse step to compensate for residual strain and to localize major treading dislocations in the M-buffer. The rate of In% change in the graded layer and in the inverse step, as well as the total buffer thickness was calculated based on the work of Y. Cordier and D. Ferre [1] for complete compensation of residual strain in M-buffers.

This approach was then extended to an InAlGaAs quaternary M-buffer scheme where the Ga% was chosen to be low enough to keep the M-buffer fairly resistive. M-buffers with 25%Ga and 75%Al grown at substrate temperature ($T_{sub}$) of 400 °C was found to exhibit extremely rough surface, possibly due to phase separation in the quaternary alloy. Reducing the starting Ga% from ~25 to ~12% and grading the In%, Ga% and Al% simultaneously was found to alleviate this problem. The grading scheme was designed such that the energy gap of the quaternary alloy remained constant and close to that of InAlAs lattice-matched to InP. Significant improvement in surface morphology was also observed when the growth temperature was lowered from 400 to 350 °C together with a slight reduction in the V/III ratio. Two different grading procedures were tested for InAlGaAs M-buffer growth: (1) continuous In grading (3→53%) and (2) In overshoot (3%→63%) plus inverse graded step (63→53%). Structures with continuous In grading exhibited superior surface morphology but slightly lower 300K and 77K mobilities.

In general, the electrical transport properties of As-based MHEMT were found to comparable favorably with those of the reference LM-HEMT structures. We observed an increase in the channel charge density of up to 29% for As-based MHEMTs with respect to reference LM-HEMTs with the same Si doping concentration. Since the reference structures were grown in between the MHEMTs, we believe this charge enhancement effect was not related to any instabilities of the Si doping concentration or InGaAs growth rates. Optimized MHEMTs incorporating an InAlGaAs quaternary buffer layer and an inverse graded step displayed excellent transport properties, even better than those grown on ternary M-buffers. 300K and 77K Hall mobilities were 10320 and 37940 cm$^2$/V-s, respectively, with an associated sheet charge of $3.0\times10^{12}$ cm$^{-3}$. Annealing of the M-buffer layer prior to active layer growth was found to have a positive effect on the 77K Hall mobility.

All MHEMT samples studied were found to exhibit orthogonal corrugations aligned along the <110> directions. Figure 2 shows a 20µm×20µm AFM scan of a quaternary InAlGaAs MHEMT, which illustrates a typical surface. This type of surface morphology, commonly known as cross-hatching, is well known to be correlated to strain relieving dislocations at the interfaces, and is the primary source of roughness in strain-relaxed metamorphic layers.

Cross-hatch patterns on the surface are common for metamorphic devices grown on GaAs and InP. Surface roughness depends not only on the total dislocation density but also on epilayer thickness, grading procedure, growth temperature, and alloy composition in the buffer. The surface morphology was monitored during growth using RHEED and visual inspection. Two-dimensional RHEED patterns with superstructures were observed at the end of the growth of all M-buffers. The development of cross-hatch patterns during the growth of As-based M-buffers was observed when the In% in the layers reached ~35–40%. Haze on the surface developed rapidly at the end of the graded layers and during the growth of the inverse step. Structures with M-buffers grown at low temperature followed by annealing exhibited better haze than those with the inverse step grown at higher temperature.

AFM data indicated that the smoothest surfaces occurred for InAlGaAs M-buffers grown at 350 °C that include an inverse graded step. This inversion layer is believed to increase the amount of strain relaxation in the buffer layer. InAlGaAs M-buffers grown at 350 °C without the inversed step also exhibited relatively low RMS values (30–39 Å for a 20μm×20μm scan). Samples grown at 400 °C, however, resulted in the worst RMS values in the series studied (>50 Å). InAlAs M-buffers generally had higher RMS values compared to the best InAlGaAs M-buffers, in agreement with published results [2]. Note that the reduction in surface roughness is often accompanied by an anisotropic distribution of cross-hatch patterns.

FIGURE 2
20μm×20μm AFM SCAN OF AN InAlGaAs MHEMT SHOWING A RIDGE-LIKE MORPHOLOGY (RMS ROUGHNESS=39.0 Å).

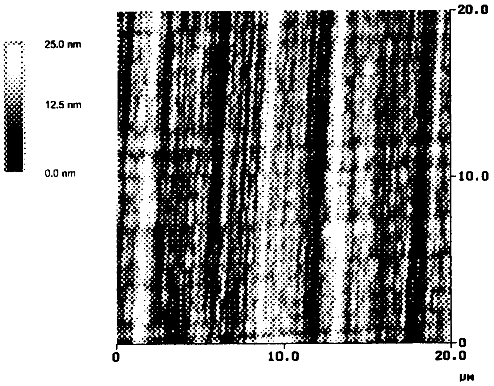

Apparently, the RMS values reported here are somewhat higher than the best values reported in the literature. However, this is most likely due to differences in how the measurement was performed. The RMS values quoted here were taken from 20μm×20μm scans. RMS measurements of the same samples taken from a scan size of 5μm×5μm generally resulted in much lower RMS values. This discrepancy is mainly due to the fact that there is correlated roughness on the surface that has a longer wavelength than 5 μm. As shown in Fig. 2, the morphology of this sample exhibits the characteristic corrugations along the <110> but the density of these corrugations is highly anisotropic. Furthermore, there appears to be a series of deep trenches and ridges that appear approximately every 7 μm. A two-dimensional power spectral density of the 20μm×20μm image shows that the transition between correlated roughness and the frequency independent regime occurs around 7 μm for this sample. RMS measurements for this sample on scan sizes below 7 μm will therefore be strongly dependent on the scan size.

Ideally, RMS measurements should only be performed on scan sizes well within the frequency independent regime. Alternatively, the scan size should be reported in tandem with RMS values. Taking this into account, the best value reported in this study is not only a more accurate assessment of the RMS roughness, but compares very favorably to the 20 Å figure of merit which was based on smaller scan sizes. Figure 3 shows (a) 20μm×20μm and (b) 5μm×5μm images for a quaternary InAlGaAs MHEMT sample. The measured RMS roughness for the large scan is 23.8 Å, the lowest for As-based M-buffers. The RMS roughness of the smaller scan is 13.9 Å, well below the target 20 Å value. This particular MHEMT structure also exhibit the highest 77K mobility (μ=37,937 $cm^2$/V-s) for a sheet charge density of $3{\times}10^{12}$ $cm^{-2}$. However, it is not entirely clear whether RMS roughness is the single mitigating factor in MHEMT performance.

FIGURE 3
(a) 20μm×20μm AND (b)5μm×5μm IMAGES OF AN InAlGaAs MHEMT. THE RMS ROUGHNESS IS 23.8 Å AND 13.9 Å, RESPECTIVELY.

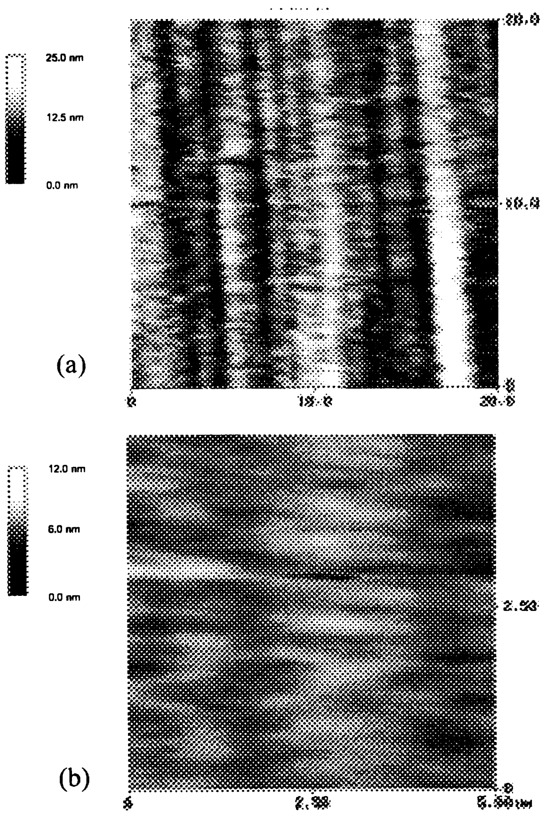

Room temperature PL mapping was used to evaluate material quality and wafer uniformity. We observe comparable PL intensity and FWHM values for MHEMT and InP HEMTs, indicative of effective dislocation filtering without the introduction of non-radiative recombination sites. A full 3" As-based MHEMT device was found to exhibit high uniformity with variation in PL wavelength and FWHM of 0.1 and 6.2%, respectively.

### (B) P-BASED MHEMT

The P-based M-buffer studied in this work is consisted of a 1.1 μm InAlP layer with a linearly graded composition of In from ~47% (lattice-matched to GaAs) to 100%. The electrical transport properties and surface morphology of InAlP-based MHEMTs was found to be comparable to that of the LM-HEMT reference, but not as good as the As-based MHEMTs. 300K and 77K Hall mobilities close to 10000 and 33000 $cm^2/V$-s, respectively, were obtained with an associated sheet charge of $2.4\times10^{12}$ $cm^{-3}$. Similar to the As-based MHEMT, a charge enhancement effect (~10%) was also observed in the InAlP-based MHEMT. While the HRXRD spectra for InAlP-based structures exhibited fairly sharp alloy peaks, the RMS roughness is barely below 60 Å. The relatively poor surface morphology is not surprising though, given the fact that we have not done any optimization of the growth parameters for this buffer scheme yet. Potentially, however, the development of P-containing ternary and quaternary alloys is useful not only for M-buffers, but also for spacer / barrier layers to increase the Schottky barrier height in high power devices.

### (C) Sb-BASED MHEMT

A 2.1 μm thick AlGaAsSb M-buffer with step-graded Sb concentration was designed to achieve complete strain relaxation from the GaAs lattice constant to the target value in the $In_{0.53}Ga_{0.47}As$ channel [2].

For a sheet charge of $3.3\times10^{12}$ $cm^{-3}$, we obtained Hall mobilities close to 9000 and 24000 $cm^2/V$-s at 300K and 77K, respectively. These values were comparable to those obtained from a reference LM-HEMT sample. A 20μm×20μm AFM scan for a typical Sb-based MHEMT is shown in Fig. 5. The RMS surface roughness of 13 Å measured is in general slightly lower than those achieved with As-based M-buffers. This can be a very attractive feature since improved MHEMT device reliability is generally associated with low surface roughness. On the other hand, the complicated grading procedure, potential cross-contamination with Sb, and the unavailability of high capacity valved Sb source may hinder the transfer of Sb-based MHEMT technology to multi-wafer MBE reactors for large volume production.

## DEVICE CHARACTERIZATION

InAlAs-based MHEMT devices were fabricated with 0.15 μm gates and source-drain spacing of 2 μm. Au/Ge/Ni/Au metallization was used for source-drain ohmic contacts. The gate metallization was Ti/Pt/Au. Initial DC measurements were performed on InAlAs-based MHEMT devices with a 2×50 μm gate periphery. A peak transconductance of 710 mS/mm was obtained at $V_{gs} = 0.05$ V. The maximum current and gate-drain breakdown voltage were 500 mA/mm and 5 V, respectively.

FIGURE 5
20μm×20μm AFM IMAGE OF AlGaAsSb M-BUFFER
(RMS ROUGHNESS = 12.9Å).

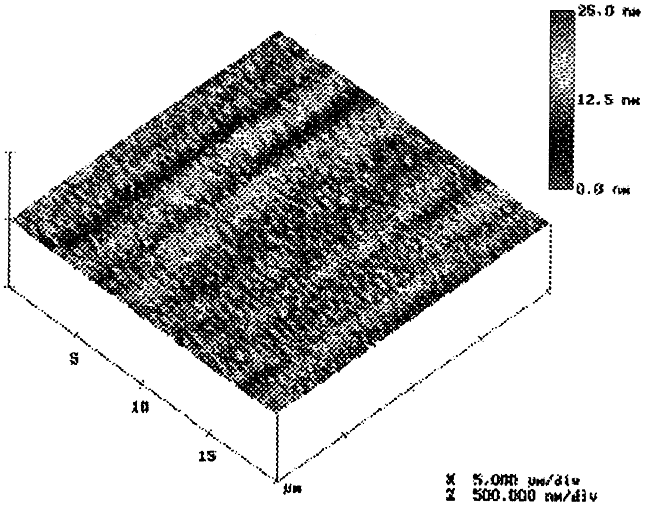

## CONCLUSIONS

In conclusion, we presented surface morphology and electrical transport data of InAl(Ga)As, InAlP and AlGaAsSb-based MHEMTs. All three MHEMT structures exhibited good electrical transport properties, with 300K and 77K Hall mobilities comparable to those obtained from reference LM-HEMT structures. RMS surface roughness less than 14 Å based on 5μm×5μm AFM scans were achieved for both InAl(Ga)As and AlGaAsSb M-buffers. InAlAs-based MHEMT devices with 0.15 μm gate was successfully fabricated with peak transconductance of 710 mS/mm, maximum current of 500 mA/mm, and gate-drain breakdown of 5 V.

## ACKNOWLEDGEMENTS

This work was partially supported by the US Army Research Laboratory under Grant No. DAAD17-99-C-0086.

## REFERENCES

[1] Y. Cordier and D. Ferre, J. Crystal Growth, **201/202**, 263 (1999).

[2] W. Hoke, P. Lyman, J. Mosca, C. Whelan, and A. Torabi, presented at the 18th NAMBE, Banff, Canada, Oct. 10–13, 1999.

[3] K.C Hwang, P.C. Chao, C. Creamer, K.B. Nichols, S. Wang, D. Tu, K. Kong, D. Dugas, and G. Patton, IEEE Elec. Dev. Lett., **20**, 551 (1999).